2019

Development of a Nanodrop Shape Analysis Tool for Installation in a Novel Nanodrop Spectrophotometer

Colin Monaghan
Technological University Dublin

Jane Courtney
Technological University Dublin, jane.courtney@tudublin.ie

Recommended Citation

Monaghan, A. & Courtney, J. (2019). Development of a nanodrop shape analysis tool for installation in a novel nanodrop spectrophotometer. *IMVIP 2019: Irish Machine Vision & Image Processing*, Technological University Dublin, Dublin, Ireland, August 28-30. doi:10.21427/w1yt-9d51

Development of a Nanodrop Shape Analysis Tool

for Installation in a Novel Nanodrop Spectrophotometer

Colin Aidan Monaghan, Jane Courtney

School of Electrical & Electronic Engineering
Technological University Dublin, Ireland
colinaidanmonaghan@gmail.com, jane.courtney@tudublin.ie

Abstract

The rapid identification of liquid composition is an important task integral to a wide range of industries including medical, pharmaceuticals, petrochemicals, and vinification. To aid in this identification spectroscopy can be utilised, however specialised instrumentation must be developed to deliver quantitative information. A spectrophotometer uses spectral data to identify chemical composition of droplets. However, to accurately perform this function, prior knowledge of the size and shape of the droplet is essential to understand chemical quantity. Whilst image data can be easily captured with a high definition camera, the image analysis to translate images into a relevant region of interest (ROI) and to extract usable data autonomously has proven challenging. Here we report the autonomous detection of nanodrops and extraction of their cartesian co-ordinates facilitating the mathematical approximations that can beget values such as volume, contact angle, rate of absorption of spectra, and the length of light paths within the medium.

Keywords: Shape Analysis, Image Processing Applications, Volume Approximation

1 Introduction

This work aims to isolate the curvature of the droplet in the form of cartesian co-ordinates and relevant variables that will allow for mathematical analyses. The initial phase was to decide on a suitable setup to acquire photographs from which all algorithms would be tested. A Raspberry Pi was connected to a camera module, and also a Sartorius 3-point scale that would assist in validating mathematical models.
Using Python with OpenCV the images were then reduced to binary values of black and white where they could be further optimised via noise removal. Using these binary images, it was possible to compare images with a rudimentary machine learning approach. From this it was possible to accurately isolate the droplet shape in an efficient and clean manner. Further variables were then extracted from the ROI that allowed for mathematical derivation that produced 3D approximations proving axisymmetry and allowed for the calculations of droplet volumes.

2 State of the Art

The flowchart shown below in Fig. 1 is the general procedure of Axisymmetric Drop Shape Analysis (ADSA) for the determination of characteristics such as the contact angle, surface area, volume, and apex curvature. ADSA (Saad & Neumann, 2016) essentially lays out the process for procuring droplet characteristics via the Young-Laplace Equation that can be mathematically manipulated (1).

$$\Delta P = \gamma \left(\frac{1}{R_1} + \frac{1}{R_2} \right) \tag{1}$$

Where R_1 and R_2 are the principal radii of curvature, the ΔP is the pressure difference across the interface, and γ is the liquid fluid interfacial tension.

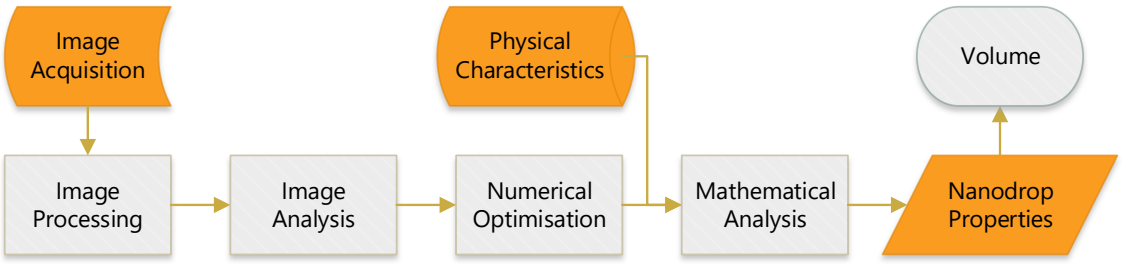

Figure 1 – General Procedure of ADSA

A specific application [Tomminen, et al., 2017] was aimed at the reactive extraction of copper in organic droplets, it approaches this from a detailed image processing perspective including video capture of moving droplets. They are attempting to isolate copper droplets within other liquid mediums. They achieve this by isolating the copper location by screening the image for colours in the red channel of the RGB spectrum. They then proceed to crop, binary threshold and reduce noise via dilation and erosion. They were additionally able to characterise their shapes by fitting ellipses and validating against samples analysed with spectrophotometry.

Calculating the volume of droplets on micro-grooved/patterned surfaces aluminium surfaces that exhibit parallel grooves such as those often found in air-cooling apparatus such as air conditioners [Sommers & Jacobi, 2008] also delved into volume calculating methods. It requires two images taken at 0° and 90° due to the elongation of the droplets caused by resting in the troughs between the micro-grooves, and gravity. Fundamentally this relies on the parallel-sided nature of water to perform volume approximations from both images to approximate a true volume.

Figure 2 - 90° and 0° Profile Respectively

Due to the unusual wetting characteristics of these surfaces the Young Laplace method wasn't a suitable characterisation of the profiles exhibited. For the 0° profile it was possible to use a volume cap method as outlined in the equation below (2).

$$V = \frac{\pi D^3}{24}\left(\frac{2-3\cos\theta+\cos^3\theta}{\sin^3\theta}\right) \quad (2)$$

Where D is the diameter, and Θ is the contact angle. However, this quickly degenerates the more the droplet elongates. Thus the 90° profile is causing the error to increase on an exponential trend. The decided methodology was to treat the droplet as a cylindrical element and integrating the cross section of the 90° profile using a series of mathematical approaches beyond the scope and application of this project.

3 Proposed Approach

The practical considerations in data gathering were an integral component of the project. Firstly, we required in order to have both images of sufficient quality to analyse. Secondly, we required accurate gravimetric measurements to compare algorithmic calculations to. During the course of our study it was realised that several parameters needed to be optimised. It was necessary to reduce disturbances generally while gathering the data, as there were many factors that could affect the scales while gathering image samples. Elements such as air conditioning, sudden changes in room pressure and temperature caused by the opening of a door all yielded sudden and dramatic fluctuations in the scales. Cautions were taken to reduce these stimuli to a minimum during the performance of each hour long experiment to ensure an optimal level of accuracy from the Sartorius scales.

The initial step was to build a database of images with corresponding weights. This would allow empirical validation of further methods developed. A Sartorius Analytical Scales 0749C range was used. Although readability of this scale is within the 0.1 mg range, however its accurate operational weighing range is unavailable. However more modern

balances have reported operational ranges above 8.2 mg with a ±0.5 mg error. Minimum and maximum values were recorded in order to offset these potential issues.

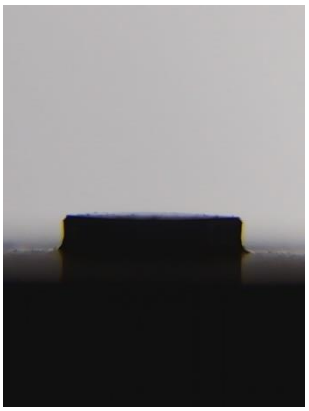

Figure 3 – Plinth

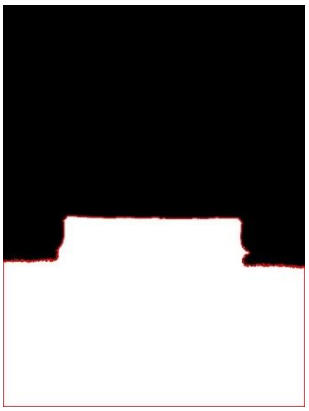

Figure 4 – Plinth Contour

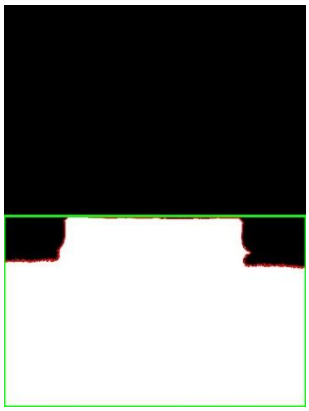

Figure 5 – Bounded Contour

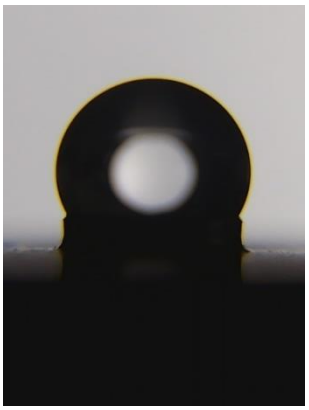

Figure 6 – Drop

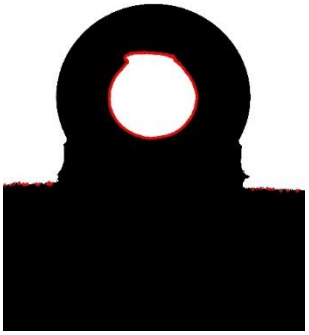

Figure 7 – Noise Contours

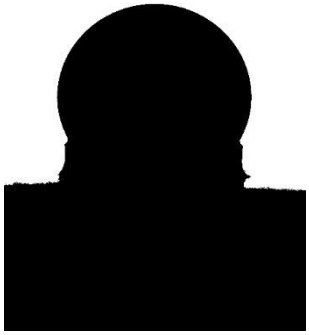

Figure 8 – Noise Filled

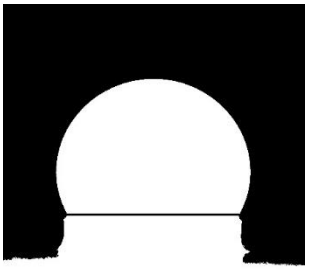

Figure 9 - Bisected

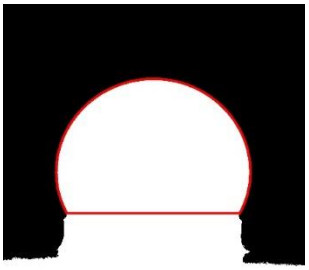

Figure 10 – Drop Contour

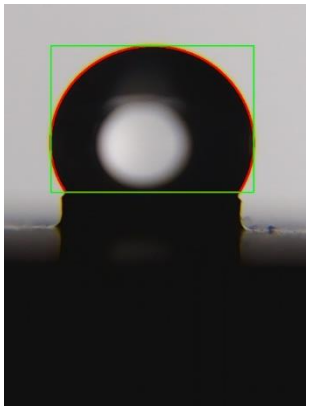

Figure 11 – Image Output

Drop staging and positioning was also important in order to create a spherical nature sans meniscus, thus the droplet was placed in a sessile constrained position on a plinth. The droplets were weighed by a four point Sartorius scale for each photograph taken. However, the droplets of interest were between 0.1 µL and 5µL and weight ranging between 0.1 mg to 5 mg ±0.5 mg error.

The most suitable approach to gathering images was to position a lightbulb producing white light behind the droplet in order to “drown out” any background spectra. By having a strong light source, it forced the internal mechanisms of the camera to scale all light by the strongest light source and weakest light source. This is how cameras produce contrast. This resulted in a ROI that was sufficiently black, with a background that was sufficiently white. Effectively this method overloads the ability of the camera to create real contrast over a range of spectra and reduced the image to two extreme parallels.

In order to process the images an initial methodology was tested that compared two images, one of the plinth sans droplet, and another with a picture of a droplet for analysis. This is to allow for comparison and identification of what is different between the pictures, i.e. the droplet.
The images are converted to grayscale (figure 3 and 6 respectively). Due to the high contrast in the images produced a wide array of threshold values are suitable. The median between the lightest and darkest pixel is selected, and using this a mask is applied to the images. Any bodies of white are then located within the image using a contour function within openCV (figure 4 and figure 7), all but the largest contour are filled in (figure 8). The contour co-ordinates of the plinth image (figure 5) are then mapped onto the droplet image and a line drawn, this effectively bisects the drop from the plinth with a line one pixel wide (exaggerated in figure 9). This line is also shifted to ensure that it bisects in the domain of the plinths pixels, and not within the pixels of the droplet itself. This could also be achieved by cropping the image to completely remove the plinth from the image. Once bisected there is now two areas that can be mapped, of which the co-ordinates from figure 10 are then exported into excel.
The plinth measured 2mm in diameter, and thus upon measuring the pixels of the plinth it is possible in each image to scale that number of pixels by 2mm, giving a real world measurement. This allowed for the height of the drop and the length of its chord to be measured in pixels and converted to mm. Once all the XY co-ordinates are recorded they are moved to the true origin (0,0) that is central to the chord of the drop.

3.7 Spherical Cap Volume Calculation

This method is mathematically exact to the conditions propagated in the images, in that it takes a sphere and can remove an amount above or below a chord (where the plinth and the droplet meet). It is essential to find the radius of the circle (3) that the droplet would be composed of if it were a full sphere. The radius can be found via the equation below, as the image is two dimensional it is easy to treat the data as circular rather than spherical:

$$r = \frac{h}{2} + \frac{c^2}{8h} \tag{3}$$

It proposes that the volume of a spherical cap equals to the sum or difference of the spherical cap and the circular cone depending on whether h < r or h > r (4)(5).

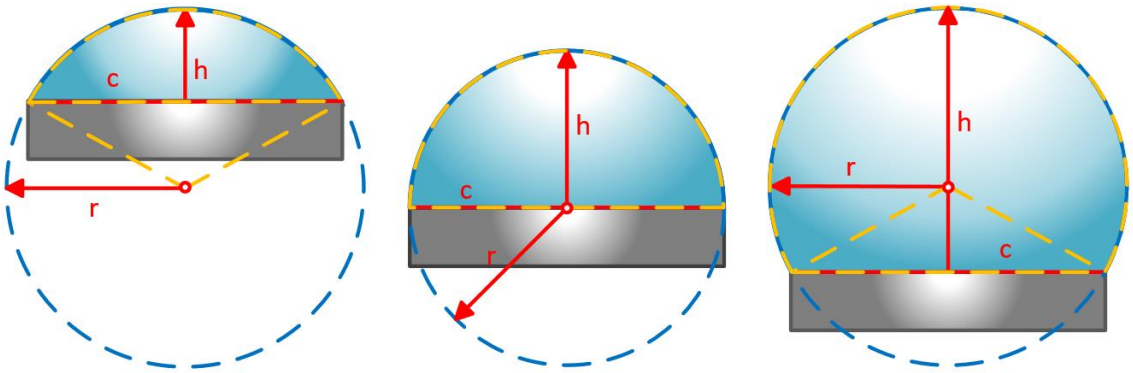

Figure 12 – Spherical Cap Method Showing Spherical Arc & Cone

$$V = \begin{cases} \pi h^2 \left(r - \frac{h}{3}\right) + \frac{1}{3}\pi a^2 (r - h) \; when \; h < r \\ \pi h^2 \left(r - \frac{h}{3}\right) - \frac{1}{3}\pi a^2 (h - r) \; when \; h > r \end{cases} \tag{4}$$

$$where \; a \; is \; the \; area \; of \; the \; circular \; chord$$

These two formula can be algebraically reduced and both will equal to the equation below:

$$V = \pi h^2 \left(r - \frac{h}{3}\right) \tag{5}$$

3.8 3D Approximation

A focal point, as discussed in chapter 3.2; needed to be isolated to facilitate the 180° rotation of the y co-ordinates into the z-domain. Using trigonometry, it is possible to approximate y and z values as they are rotated around the origin (6).

The following adjustments were made iteratively to every co-ordinate and mapped for the length of the radians array, while also using the radians array to dictate the rotations. In the original Cartesian format, the z-domain is at *(x, y, 0)* as the z-values are realised only at value *0*.

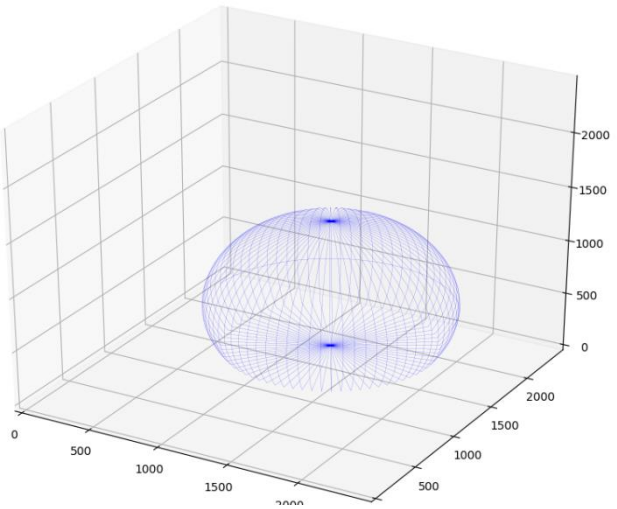

Figure 13 – 3D Droplet Via Reverse Plotting

$$(x,y,z)\begin{cases} x = x[n] - O_x \\ \mathrm{y} = (\sin\theta)\,(z[n]) + (\cos\theta)(y[n] - O_y) \\ \mathrm{z} = (\cos\theta)(z[n]) - (\sin\theta)\,(y[n] - O_y) \end{cases} \quad (6)$$

Where O_x and O_y are the Cartesian origin co-ordinates, and *[n]* all of the values stored in the co-ordinates arrays; iterated one at a time. The x and y co-ordinates were adjusted to reflect the true origin that was mapped onto the centre of the chord, this was required as the equation above is only suitable for rotations around an origin.

4 Results & Analysis

4.1 Contour Approximation for X-Y Co-ordinates

As demonstrated below from Fig. 14 through Fig. 19 the droplet shape is recognised from the input. Drop shape and location has no impact on the algorithm so long as there is a plinth photograph as part of the input for ROI identification.

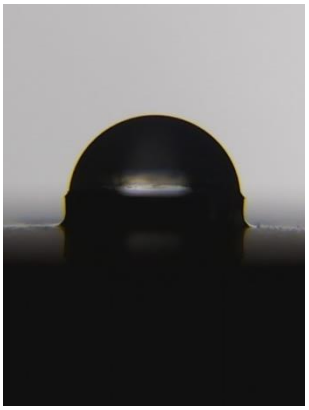

Figure 14 – Typical Input

Figure 15 – Unrealistic Input

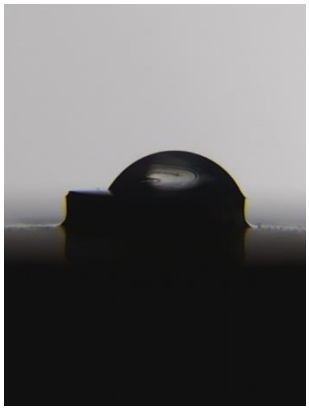

Figure 16 – Shifted Input

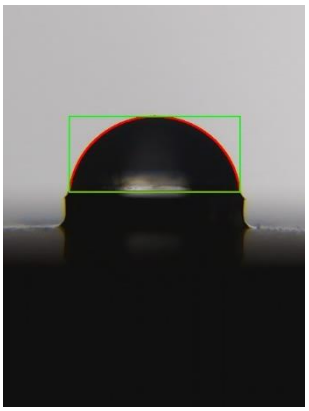

Figure 17 – Typical Output

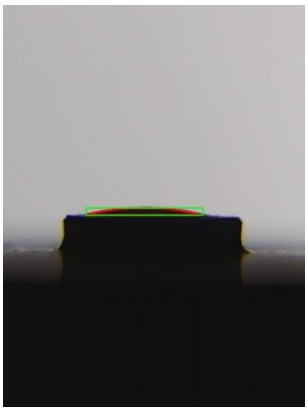

Figure 18 – Unrealistic Output

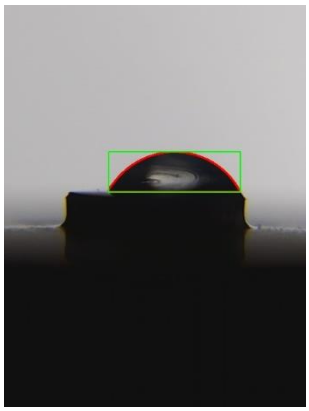

Figure 19 – Shifted Output

4.2 Volume Approximation

The main mechanism of the algorithm is that it compares a picture of a drop to a picture of a plinth. In order to avoid moving the plinth due to the prototype stage of the equipment, the easiest methods to take pictures was to allow them to evaporate over time and take images at intervals. The error of the Sartorius scales used in an ideal environment is ± 0.5mg. However, as the doors on the device were not closed in order to facilitate the camera this error would be expected to increase.

Due to an unideal weighing environment, the scales tended to oscillate ±1mg several times over the course of the minute between each image capture. This oscillation adds an additional error to the 0.5 mg which is integral to the balance. Halfway through this experiment the min and max values showcased on the scales were recorded for analysis.

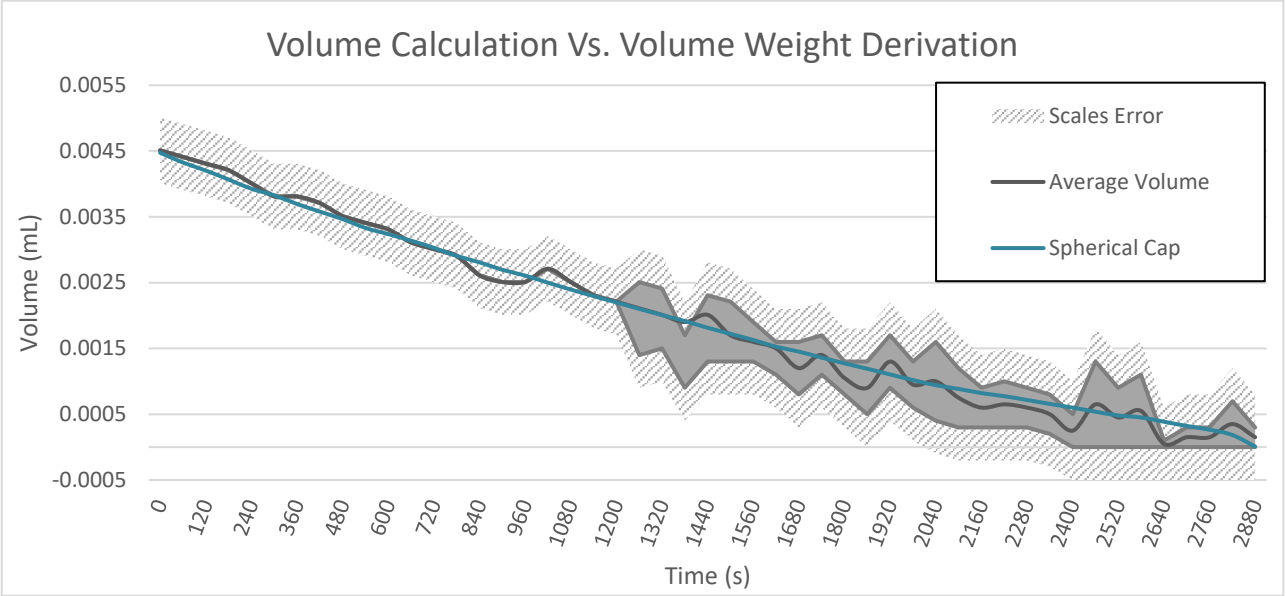

Graph 1 - Evaporation Data Trend (Scales Weight Vs. Spherical Cap Calculation)

As shown in Graph 1 there is a wide degree of oscillation in weighed values as measured from 1200(s). The origin of this increased error is a higher degree of variation caused by measuring these lower weights in a non-ideal environment

At 2280 (s) the trend recording the volume approximations is disrupted. When the pictures produced from this time onwards are inspected it is due to uncontrolled slipping of the contact line of the droplet causing the edge of the droplet to recede from the edge of the plinth.

As the droplet shrinks in diameter, its surface area decreases in respect to its overall volume, thus giving it less contact with surrounding air to allow evaporation to occur. This would cause the volume to remain constant for longer, as graph 1 indicates using the volume approximation methods devised.

This had to be taken into consideration in the design of the algorithm, as previously the chord and scaling variables were identical. It was presumed that the drop would always wet the full plinth. Thus the scaling of the picture was adjusted to be iteratively based off of the first contour (the plinth itself), instead of the second longest contour (the droplet).

This also pointed out issue with the plinth itself, while all care was taken to remove any oil, or residue before the experiment; if this were done correctly the above droplet trend would not have occurred. While the plinth could be coated to make it hydrophobic or oleopathic this would overall affect the data gathering negatively. The plinth is designed to be wetted fully by the liquid, making it hydrophobic deters this. While making it oleopathic would reduce oil or grease from fingertips, it means these types of liquids couldn't be measured by the device.

5 Conclusions & Future Work

The spherical cap method has been demonstrated as a reliable approximation method for sessile droplets. Allowing for the calculation of their shape and volume, calibrated by gravimetric analysis. Whilst these results would benefit from a graduated calibration method, this proof of principle study demonstrates the potential for data extraction from sessile droplets through image analysis. With these results in hand, future work would seek to combine these measurements with spectrophotometry. Such efforts would allow for the calibration of absorption spectra and light paths within the medium, providing quantification of the droplets contents. Ultimately we hope that this technology will find application and integration with biomedical devices examining real world analytes in a human health context.

References

[Bortolotti et al., 2009] Bortolotti, M., Brugnara, M., DellaVolpe, C. & Siboni, S., (2009). *Numerical Models for the Evaluation of the Contact Angle from Axisymmetric Drop Profiles: A Statistical Comparison*. Journal of Colloid & Interface Science, Issue 336, pp. 285-297.

[Cabezas et al., 2007] Cabezas, M. G., Montenaro, J. M. & Ferrera, C., (2007). *Computational Evaluation of the Theoretical Image Fitting Analysis—Axisymmetric Interfaces (TIFA-AI) Method of Measuring Interfacial Tension*. Measurement Science & Technology, 18(5).

[del Rio & Neumann, 1997] del Río, O. I. & Neumann, A. W., (1997). *Axisymmetric Drop Shape Analysis: Computational Methods for the Measurement of Interfacial Properties from the Shape & Dimensions of Pendant & Sessile Drops*. Journal of Colloid & Interface Science, Issue 196, pp. 136-147.

[ElSherbini & Jacobi, 2004] ElSherbini, A. I. & Jacobi, A. M., (2004). *Liquid Drops on Vertical & Inclined Surfaces II. A Method for Approximating Drop Shapes*. Journal of Colloid & Interface Science, Issue 273, pp. 566-575.

[Farshid & Amirfazli, 2011] Farshid Chini, S. & Amirfazli, A., (2011). *A Method for Measuring Contact Angles of Asymmetric and Symmetric Drops*. Colloids & Surfaces A: Physicochemical Engineering Aspects. s.l.:Elsevier, pp. 29-37.

[Farshid & Neumann, 2006] Hoorfar, M. & Neumann, A. W., (2006). *Recent Progress in Axisymmetric Drop Shape Analysis (ADSA)*. In: Advances in Colloid & Interface Science. s.l.:Elsevier, pp. 25-49.

[Iliev & Pesheva, 2006] Iliev, S. & Pesheva, N., (2006). *Nonaxisymmetric Drop Shape Analysis and its Application for Determination of the Local Contact Angles*. *Journal of Colloid & Interface Science, Issue 301, pp. 677-684.*

[Saad & Neumann, 2016] Saad, S. M. & Neumann, A. W., (2016). *Axisymmetric Drop Shape Analysis (ADSA): An Outline*. In: Colloids & Surfaces A: Physiochemical & Engineering Aspects. s.l.:Elsevier, pp. 62-87.

[Sommers & Jacobi, 2008] Sommers, A. & Jacobi, M. A., (2008). *Calculating the Volume of Water Droplets on Topograhically-Modified, Micro-Grooved Aluminium Surfaces.* Purdue, s.n.

[Srisha & Khan, 2015] Srisha, R. & Khan, A., (2015). Morphological Operations for Image Processing: Understanding and its Applications. s.l., s.n.

[Tahseen et al., 2017] Tahseen, K. et al., (2017). *Design and fabrication of a passive droplet dispenser for portable high resolution imaging system*. Scientific Reports, Volume 7, p. 41482.

[Tomminen et al., 2017] Tomminen, J. et al., (2017). *Determination of single droplet sizes, velocities and concentrations with*. Chemical Engineering Science, Issue 167, pp. 54 - 65.